Insight For The Construction of R-T Phase Boundary in KNN Piezoceramics From The View of Energy Band Structure

Xingcheng Wang
Guizhou University
Cheng Meng
East China University of Technology
Y.Y. Wang (yuanyuwang0216@163.com)
Guizhou University

Research Article

Keywords: Piezoceramics, MPB, R-T phase coexistence, Energy band structure, hybridization

Posted Date: April 14th, 2021

DOI: https://doi.org/10.21203/rs.3.rs-416212/v1

Abstract

The crystal structures and associated energy band structures of classic lead-based PZT ($PbZr_{0.5}T_{i0.5}O_3$) and lead-free KNN ($K_{0.5}Na_{0.5}NbO_3$) piezoelectric ceramics prepared by a solid-state method are systematically studied based on the First-principles calculations. For better understanding relations between energy band structures and the phase structures in the PZT and KNN, the components PT (PbT_iO_3)/PZ ($PbZrO_3$) and KN ($KNbO_3$)/NN ($NaNbO_3$) are also calculated. The results suggest that the vital contribution to R-T morphotropic phase boundary (MPB) in PZT comes from the hybridization of A-site and B-site ions, which causes stretching and tilting of oxygen octahedron and therefore leads to the formation of R and T phases. The KNN behaves differently. Moreover, it's concluded that the band structure highly inherited from tetragonal PT plays an important role in the construction of the R-T phase boundary according to the comparison of PZT and KNN. In general, the work inspires an idea from the view of energy band structure to realize R-T phase coexistence as well as improved piezoelectric properties in KNN-based lead-free piezoceramics.

Introduction

Lead zirconate titanate is a widely used piezoelectric ceramic that can transfer mechanical and electrical energy. With an increasing awareness of sustainable development, lead-free piezoceramics, especially KNN with high Curie temperature (T_c), has attracted more and more attention [1–3]. However, the electrical properties of KNN piezoceramics are inferior to PZT-based ones. Through dopant modification and advanced synthesis methods, the properties of KNN piezoceramics are enhanced dramatically and even reach comparable values to commercial PZT-5H and PZT-5A [4, 5]. The polymorphic phase boundary (PPB) and nano ferroelectric domains are regarded as key factors to property enhancement, and they are closely related to the dopants [6]. Nevertheless, the effects of the dopants on phase structure as well as property enhancement are rarely mentioned from the view of energy bands. It's worth noting that both the PZT and KNN consist of ferroelectric materials (i.e. PT and KN) and anti-ferroelectric materials (i.e. PZ and NN), but their phase structures and electrical properties are different [7, 8]. It's well known that the lattice deformation and associated phase transition are closely related to electrons' states and their interactions. Therefore, research on the energy band structures and the density of states for PZT and KNN probably opens up a new horizon to explain the differences between PZT and KNN, and makes a good start to help us understand the effects of dopants on phase structure and property enhancement [9, 10].

Density functional theory (DFT) is an important method for studying the ground-state theory of multiparticle systems. The basic idea is that the physical properties of the ground state of atoms, molecules and solids can be described by the particle number density function, and the ground state of the system is the state in which the energy functional takes the minimum value under the condition of constant particle number.[11, 12] This not only provides a theoretical basis for simplifying the multi-electron problem into a single electron problem but also does not need to rely on any empirical parameters. The atomic and electronic structures and related physical properties of materials can be obtained by solving the intrinsic quantum mechanical equations. It provides a direct and effective method for studying the relationship between microstructure and macroscopic properties of materials [13].

By using the super-soft pseudopotential method, this pseudopotential introduces an overlap operator to plane wave, which reduces the plane-wave basis function. To solve the problem of large modulus conservation, this method is employed [14]. Generally speaking, the calculation of the pseudopotential method is small, in which the inner electronic state is eliminated, and an approximation is introduced more than that of the all-electron method [15].

In recent years, the generalized gradient approximation (GGA) has attracted increasing attention. Compared with the traditional LDA approximation, GGA further considers the influence of the nearby charge density on the exchange-correlation energy, i.e. the influence of the first-order gradient of the charge density [16]. Generally, the GGA method can give more accurate energy and structure, which can avoid underestimating exchange energy and overestimating correlation energy when LDA is used and applied to analyze the relation between PZT and KNN [17–19].

Therefore, in the work, the energy band structure and associated electron density of PZT and KNN piezoceramics prepared by a solid-state method are systematically studied based on the First-principles calculations [20]. The Perdew Burke Ernzerhofer (PBE) is a simplified form without experimental parameters to deal with the exchange-correlation energy of the electron-electron interaction [21]. The PBE functional of general gradient approximation (GGA) was established by using the exchange-correlation energy function of electron and electron interaction. The electronic wave function was expanded based on the plane wave. The GGA with the Perdew-Burke-Ernzerhof (PBE) exchange-correlation function was used in this work. The GGA and Perdew Burke Ernzerhof (PBE) were used to deal with the exchange-correlation potential [22, 23]. The formula of the exchange-correlation energy function is written by:

$$E_{xc}[\rho] = \int f_{xc}(\rho(r), |\nabla \rho(r)|) d^3 r$$

In the formula, E_{xc} is the exchange-correlation energy and $\rho(r)$ is the local electron density for triple integration. Besides, the band structures of PT/PZ and KN/NN are also calculated to better investigate the origins of different phase structures in the PZT and KNN. Then the partial density of states (PDOS) of each matter is calculated to study the degrees of orbital hybridization and electron localization, which account for the lattice deformation as well as a phase transition. In General, the work inspires a thought to construct the R-T polymorphic phase boundary of KNN-based lead-free piezoceramics through the addition of the dopant with appropriate energy band structures.

Methods And Parameters

The investigated ceramics were prepared by the conventional solid-state reaction method. Firstly, weighed raw materials were ball-milled in a polyethylene jar using ZrO_2 balls and the anhydrous ethanol for 12 h and calcined after drying. Then the calcined powders were ball milled again for 12 h. After drying, the powders were mixed with 6% paraffin and then pressed into disc particles with a diameter of 10.0 mm and thickness of 1.2 mm under the pressure of 10 MPa. The preparation process for the above ceramics is listed in Table 1. Then, the phase of the sintered samples was detected by X-ray diffraction (XRD) with a Cu Kα radiation (Xpert-PRO, PANalytical Company, The Netherlands). The band structure was calculated using Materials Studio software (Version of CASTEP-19.11) and the Vienna ab initio simulation package (VASP) which is based on density functional theory (DFT) and the plane-wave pseudopotential methods.

Table 1
The preparation process for the above ceramics

	NN	KN	KNN	PZ	PT	PZT
Raw materials	Na_2CO_3(99.8%) Nb_2O_3(99.5%)	K_2CO_3(99%) Nb_2O_5(99.5%)	K_2CO_3(99%) Na_2CO_3(99.8%) Nb_2O_5(99.5%)	Pb_3O_4(98%) ZrO_2(99%)	Pb_3O_4(98%) TiO_2(99%)	Pb_3O_4(98%) ZrO_2(99%) TiO_2(99%)
Calcinating Temperature &Time	two-stage annealing at T = 800–850 °C for four hours (h) at each stage	625℃/4h	850℃/6h	1200℃/2h	850℃/1.5h	900℃/4h
Sintering Temperature &Time	1220–1240 °C/2h	1035℃/1h	1110℃/3h	1300℃/1h	1220℃/2h	1250℃/4h

The First-principles calculations were based on the crystal structure of the targeted material. All the calculations were carried out by the CASTEP package which was based on density functional theory (DFT) and the ultrasoft pseudopotential methods. The plane-wave cutoff energy was set at 300 eV and the convergence for energy is chosen as 2×10^{-5} eV. The accuracy of interatomic force was 0.05 eV/Å, the accuracy of internal stress was 0.1 GPa, and the accuracy of displacement tolerance was 2×10^{-4} nm. When the DFT theory of GGA was used, only the local electronic states of the outermost *s* and *p* orbits were considered, and the influence of the inner electronic states was not taken into consideration, which inevitably leads to the smaller energy gap. Even so, the differences in the band structure, the density of states of various systems were still able to reveal the origins of the R-T phase boundary in PZT [19]. Consequently, this work inspires an idea from the view of energy band structure to realize R-T phase coexistence as well as improved piezoelectric properties in KNN-based lead-free piezoceramics.

Results And Discussion

Figure 1 is the crystal structure, energy band structure and PDOS of $NaNbO_3$ (NN) piezoceramics. The space group of NN is Pmc21 (Orthorhombic phase), as shown in Fig. 1(a). Figure 1(b) gives the corresponding band structure. It's well known that the top of the valence bands (VB) and the bottom of the conduction bands (CB) are located at the same high symmetric point in the Brillouin region, suggesting that the material is a direct gap semiconductor and vice versa. Therefore, NN is a direct gap semiconductor and the forbidden bandgap (E_g) is 2.4 eV. Besides, the energy bands are compact and flat, resulting from the high degree of electron localization. The results are consistent with the PDOS in which the peaks of O 2*p* and Nd 4*d* are detected, as presented in Fig. 1(c). According to the PDOS, it's found that the energy bands are mainly ascribed to covalent interaction of O 2*p* orbit and Nd 4*d* orbit over the energy range of 2.5 eV-5 eV (for calculation convenience, we define the Fermi level as 0 eV), and the overlapped sharp peaks imply the formation of quasi *s-p* hybridized orbit between O and Nb atoms. Furthermore, the energy bands lying in the energy range of -5 eV-0 eV are also mainly attributed to Nb 4*d* and O 2*p* orbits. The hybridized orbit facilitates the formation of strong binding between adjacent atoms, which is closely related to the crystal structure. More importantly, the A-site ions, i.e. Na, are not involved in the bonding.

Fig. 2 is the crystal structure, energy band structure and PDOS of KN piezoceramics using the lattice parameters reproduced. As shown in Fig. 2(a), the space group of KN is Bmm2 (Orthorhombic phase). Fig. 2(b) is the band structure of KN. It's observed that KN is an indirect gap semiconductor since the bottom CB and the top VB lie at different positions. That means both the energy and the momentum change when the electron jumps between two energy states. Besides, as can be seen, the E_g of KN is 2.11 eV, smaller than that of NN. However, unlike NN, the CB are loosened. Fig. 2(c) is the PDOS of KN. Similar to NN, the top bands of VB (-5 eV-0 eV), are derived from the hybridization of O 2*p* orbits and Nb 4*d* orbits. Moreover, the bottom of CB at 2.4 eV-7.5 eV is mainly attributed to the Nb 4*d* orbits, different from O 2*p* and Nb 4*d* hybridization of NN. Above the bands, the PDOS is complicated. The overlapped curves corresponding to the outermost *s* and *p* orbits of elements imply that all orbits except O 2*p* are involved to constitute the conduction bands. The weak hybridization of KN accounts for the compact crystal structure of KN compared to NN and namely, the lattice volume of KN (129.402 $A(0)^3$) is smaller than that of NN (147.397 $A(0)^3$) since the hybrid orbits with specific spatial orientations restrict the degree of freedom of lattice deformation. Furthermore, the bands become loosened, indicating that the electron localization of KN weakens compared to NN.

Figure 3 is the crystal structure, energy band structure and PDOS of KNN piezoceramics using the lattice parameters reproduced. As shown in Fig. 3(a), the space group of KNN is Amm2 (O phase). It's universally acknowledged that KNN is composed of antiferroelectric NN and ferroelectric KN. However, the energy band structure of KNN seemingly inherits from NN, as shown in Fig. 3(b), since they possess similar orbital hybridization and compact energy bands. The E_g of KNN is 1.807 eV, smaller than that of KN or NN. Because the supercell which is utilized to calculate, consists of hundreds of atoms, the energy bands are dense compared to NN and KN. Furthermore, the energy band structures of KNN are seemingly comprised of those in KN and NN, and the vanished energy bands between 5eV and 15eV indicate that the orbital hybridization at the upper state of KN weakens when the KN and NN constitute KNN. On the contrary, the highly localized K 3*p* orbital of KN remains which appears at around − 10 eV.

PZT is extensively used which is also composed of antiferroelectric PZ and ferroelectric PT. However, the piezoelectric properties of PZT are superior to KNN. To explore the differences between PZT and KNN, the energy band structures and PDOSs of PZ, PT and PZT piezoceramics are calculated using the same method, as exhibited in Fig. 4. Figures 4(a1), 4(b1) and 4(c1) are the crystal structures of PZ, PT and PZT piezoceramics. It's observed that the space groups of PZ, PT and PZT are Pbam (Orthorhombic phase), P4mm (Tetragonal phase) and C1m1 (Centered monoclinic) respectively. The phase C1m1 was discovered at low temperatures along the R-T MPB according to the high-resolution x-ray diffraction study of PZT, and therefore, it's a transitional phase between the R and T phase [24–26]. Figures 4(a2), 4(b2) and 4(c2) give the energy band structures of PZ, PT and PZT ceramics. As presented in Fig. 4(a2), antiferroelectric PZ is an indirect gap semiconductor with E_g~2.4 eV. Similar to the NN, the flat and compact energy band structures are detected. Accordingly, as exhibited in Fig. 4(a3), the hybridization of Pb 6*p* and Zr 4*d* orbits plays an important role in the formation of the quasi *s*-*p* hybridized orbit at the bottom of CB within the range of 2.7 eV-4.5 eV. Nevertheless, the top of VB (-4.4 eV-0 eV) is highly attributed to O 2*p*, Zr 4*d* while Pb 6*s* and 6*p* orbits are involved to some extent. The involvement of A-site Pb and featured orbit hybridization in the bottom of CB are regarded as the origins of the R phase of PZT. Figure 4(b2) is the band structure of ferroelectric PT. It's seen that the energy band structures become loosened for PT (indirect gap semiconductor and E_g~2.2 eV). However, unlike KN, the bottom of CB is mainly derived from the hybridization of Ti 3*d* and Pb 6*p* orbits. More importantly, compared to KN, at higher CB from 8.1 eV to 14 eV, an electron-forbidden area is detected.

Concerning PZT, in the first place, the E_g (2.03eV) decreases compared to PZ and PT. As depicted in Fig. 4(c2), the synergistic effect of PZ and PT gives rise to comparably flat and compact band structures alike to KNN, since the calculated supercell is smaller than KNN. Furthermore, the band structures of PZT are highly similar to PT, as

presented in Fig. 4(b2). However, as exhibited in Fig. 4(c3), the higher CB within 8.2 eV-14.3 eV, disappear for PZT compared to PT, indicating that the effects of Ti 4*s* and Ti 3*p* vanish when the PZT is constituted.

Figure 5(a) gives the electron densities of KNN and PZT. The typical quasi *s-p* hybrid orbit is observed for KNN according to the isosurface scale. The positive isosurface represents the accumulation of charge while the negative isosurface suggests the reduction of the charge. Therefore, the linear type *s-p* hybrid orbit appears around O ions and orientates along Nb and O ions. On the contrary, the involvement of the A-site K ion for the hybridization is absent. For PZT, the hybridization of B-site Zr and Ti and O ions is investigated. However, the degree of such hybridization decreases according to the weakened color of the positive isosurface. Moreover, it's detected that the proximate region of A-site Pb ions presents the positive isosurface for accumulation of charge. The circular region implies *s* orbit exists around Pb ions. Consequently, the process of lattice deformation as well as phase transition is deduced, as exhibited in Fig. 5(b). The *s-p* hybrid orbit results in the symmetric stretching of oxygen octahedron and hence the *c* increases, resulting in the formation of the T phase. Meanwhile, the Pb ions with like charges repel each other, leading to the tilting of oxygen octahedron, and therefore the R phase forms [27–29]. For the convenient observation of the tilting, only the bendings in (000) and (001) planes are presented. The bendings in other planes are alike to the situation of (000) and (001) planes.

Therefore, the construction of the R-T phase boundary in KNN can take a cue from the PZT, that is the strengthening of the A-site ion's effect and the weakening of the B-site ion's effect. The key factors are easy to understand. Firstly, the involvement of the A-site ion gives birth to the tilting of the B-site ion. Secondly, the deformation of oxygen octahedron would be restricted to the stretching of *c* if the hybridization ability of the ion in the B site is relatively strong. Consequently, only the T phase is constructed.

Above all, a feasible strategy is proposed to obtain R-T phase boundary as well as enhanced the piezoelectric properties of KNN piezoceramics, the end members composed of the A-site or B-site dopants with appropriate hybridization ability. The hybridization ability can be reflected partly by the electronegativity which is also representative of the ability to bind the electrons. Namely, the electronegativity of dopants can be utilized to estimate the feasibility of dopant modification.

Conclusions

To understand why the phase structure of KNN differs from PZT, even though they are both constituted by the antiferroelectric and ferroelectric, the First-principles calculations of KNN and PZT as well as their components-KN and NN, PT and PZ, are conducted. The results suggest that the R-T phase boundary which is demonstrated to facilitate the property enhancement of perovskite piezoceramic is generated by the hybridization of A-site ion and relatively weakened hybridization of B-site ion. Besides, the electronegativity represents the ability of hybridization to some extent. Therefore, the electronegativity is an important consideration for the options of dopants or end members. Besides, the contents and other characteristics of dopants, such as ionic radius and valence, are also taken into consideration to construct the R-T phase boundary and obtain promoted piezoelectric properties of KNN.

Declarations

Acknowledgments

This work was supported by the National Natural Science Foundation of China (No. 51862003), and the Science and Technology Planning Project of Guizhou ([2019]1094). We also thank Prof. Wu at Sichuan University to provide

valuable suggestions to us.

References

[1] Tian H, Hu C, Chen Q*, et al.* High, purely electrostrictive effect in cubic $K_{0.95}Na_{0.05}Ta_{1-x}Nb_xO_3$ lead-free single crystals. *Mater Lett* 2012. 68:14-16.

[2] Tian H, Hu C, Meng X*, et al.* Top-Seeded Solution Growth and Properties of $K_{1-x}Na_xNbO_3$ Crystals. *Cryst Growth & Des* 2015. 15:1180-1185.

[3] Guo Y, Kakimoto K-i, Ohsato H. Phase transitional behavior and piezoelectric properties of $(Na_{0.5}K_{0.5})NbO_3$–$LiNbO_3$ ceramics. *Appl Phys Lett* 2004. 85:4121-4123.

[4] Sheeraz MA, Butt Z, Khan AM*, et al.* Design and Optimization of Piezoelectric Transducer (PZT-5H Stack). *J Electron Mater* 2019. 48:6487-6502.

[5] Singhal A, Mohammad Sedighi H, Ebrahimi F*, et al.* Comparative study of the flexoelectricity effect with a highly/weakly interface in distinct piezoelectric materials (PZT-2, PZT-4, PZT-5H, $LiNbO_3$, $BaTiO_3$). *Waves Random Complex Media* 2019. 20:1-19.

[6] Slater JC. Wave Functions in a Periodic Potential. *Phys Rev* 1937. 51:846-851.

[7] Sun X, Zhao C, Lv X*, et al.* Decoding the Role of Diffused Multiphase Coexistence in Potassium Sodium Niobate-Based Ceramics with Nanodomains for Enhanced Piezoelectric Devices. *ACS Appl No Mater* 2019. 3:953-961.

[8] Zhou SL, Zhao X, Jiang XP*, et al.* Electronic and Optical Properties of $KNbO_3$, $NaNbO_3$ and $K_{0.5}Na_{0.5}NbO_3$ in Paraelectric Cubic Phase: a Comparative First-principles Study. *Chin J Struct Chem* 2012. 31:1095-1104.

[9] Chen F, Schafranek R, Li S*, et al.* Energy band alignment between $Pb(Zr,Ti)O_3$ and high and low work function conducting oxides-from hole to electron injection. *J Phys D-Appl Phys* 2010. 43:295-301.

[10] Samanta S, Sankaranarayanan V, Sethupathi K. Band gap, piezoelectricity and temperature dependence of differential permittivity and energy storage density of PZT with different Zr/Ti ratios. *Vacuum* 2018. 156:456-462.

[11] Herring, Conyers. A New Method for Calculating Wave Functions in Crystals. *Phys Rev* 1940. 57:1169-1177.

[12] Naito T, Ohashi D, Liang HZ. Improvement of functionals in density functional theory by the inverse Kohn-Sham method and density functional perturbation theory. *J Phys B-At Mol Opt Phys* 2019. 52:245003.

[13] Herring C. A New Method for Calculating Wave Functions in Crystals. *Phys Rev* 1940. 57:1169-1177.

[14] Vanderbilt. Soft self-consistent pseudopotentials in a generalized eigenvalue formalism. *Phys rev B Condens matter* 1990. 41:7892-7895.

[15] Hou QY, Liu YJ. Effect of Li doping and point vacancy on photocatalytic properties and mechanism of ZnO. *Chem Phys* 2020. 531:110657.

[16] Wu Z, Cohen RE, Singh DJ. Comparing the weighted density approximation with the LDA and GGA for ground-state properties of ferroelectric perovskites. *Phys Rev B* 2004. 70:104112.

[17] Yang D, Wei LL, Chao XL*, et al.* First-principles calculation of the effects of Li-doping on the structure and piezoelectricity of $(K_{0.5}Na_{0.5})NbO_3$ lead-free ceramics. *Phys Chem Chem Phys* 2016. 18:7702-7706.

[18] Wang T, Fan Y-C, Xing J*, et al.* First-principles calculation of influences of La-doping on electronic structures of KNN lead-free ceramics*. *Chin Phys B* 2020. 29.

[19] Li C, Xu X, Gao Q*, et al.* First-principle calculations of the effects of $CaZrO_3$-doped on the structure of KNN lead-free ceramics. *Ceram Int* 2019. 45:11092-11098.

[20] Segall MD, Lindan PJD, Probert MJ*, et al.* First-principles simulation: ideas, illustrations and the CASTEP code. *J Phys: Condens Matter* 2002. 14:2717-2744.

[21] Perdew JP, Burke K, Ernzerhof M. Generalized Gradient Approximation Made Simple. *Phys Rev Lett* 1996. 77:3865-3868.

[22] Filippi C, Umrigar C, Taut M. Comparison of exact and approximate density functionals for an exactly soluble model. *J Chem Phys* 1994. 100:1290-1296.

[23] Perdew JP, Zunger A. Self-interaction correction to density-functional approximations for many-electron systems. *Phys Rev B* 1981. 23:5048-5079.

[24] Dmowski W, Egami T, Farber L*, et al.* Structure of $Pb(Zr, Ti)O_3$ near the morphotropic phase boundary. *AIP Conf Proc* 2001. 582:33-44.

[25] Wu W, Xiao D, Wu J*, et al.* PHASE STRUCTURE, PIEZOELECTRIC AND MULTIFERRIOC BEHAVIOR OF $(K_{0.48}Na_{0.52})NbO_3$-Co_2O_3 PIEZOELECTRIC CERAMICS. *Funct Mater Lett* 2012. 04:225-229.

[26] Fu Z, Yang J, Lu P*, et al.* Influence of secondary phase on polymorphic phase transition in Li-doped KNN lead-free ceramics. *Ceram Int* 2017. 43:12893-12897.

[27] Kalem V, Cam I, Timucin M. Dielectric and piezoelectric properties of PZT ceramics doped with strontium and lanthanum. *Ceram Int* 2011. 37:1265-1275.

[28] Wang CH. The piezoelectric and dielectric properties of PZT–PMN–PZN. *Ceram Int* 2004. 30:605-611.

[29] Nasar RS, Cerqueira M, Longo E*, et al.* Experimental and theoretical study of the ferroelectric and piezoelectric behavior of strontium-doped PZT. *J Eur Ceram Soc* 2002. 22:209-218.

Figures

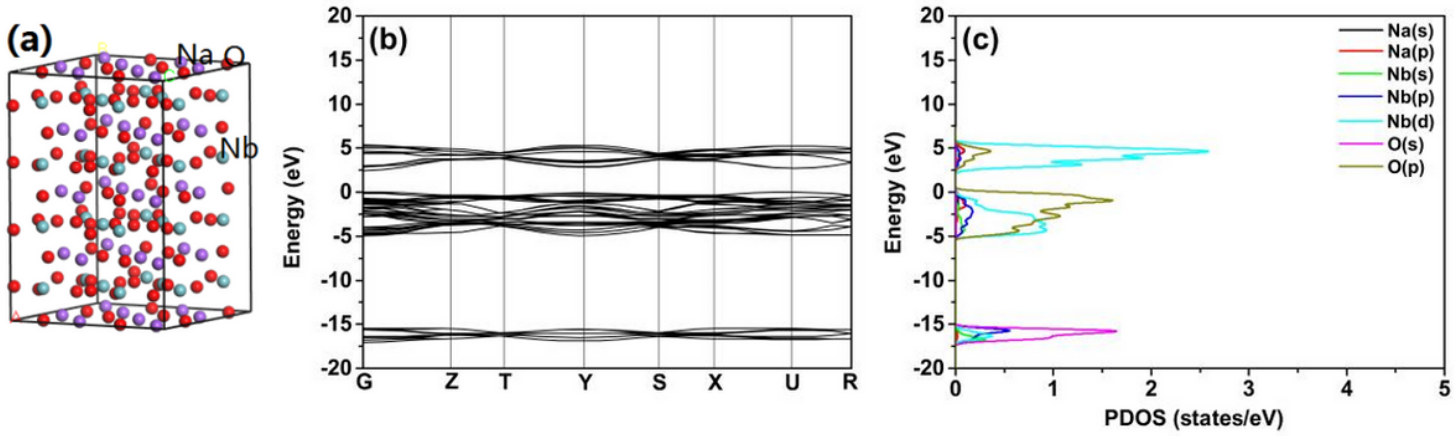

Figure 1

(a) The crystal structure; (b) the energy band structure and (c) the PDOS of NaNbO3 (NN) piezoceramics

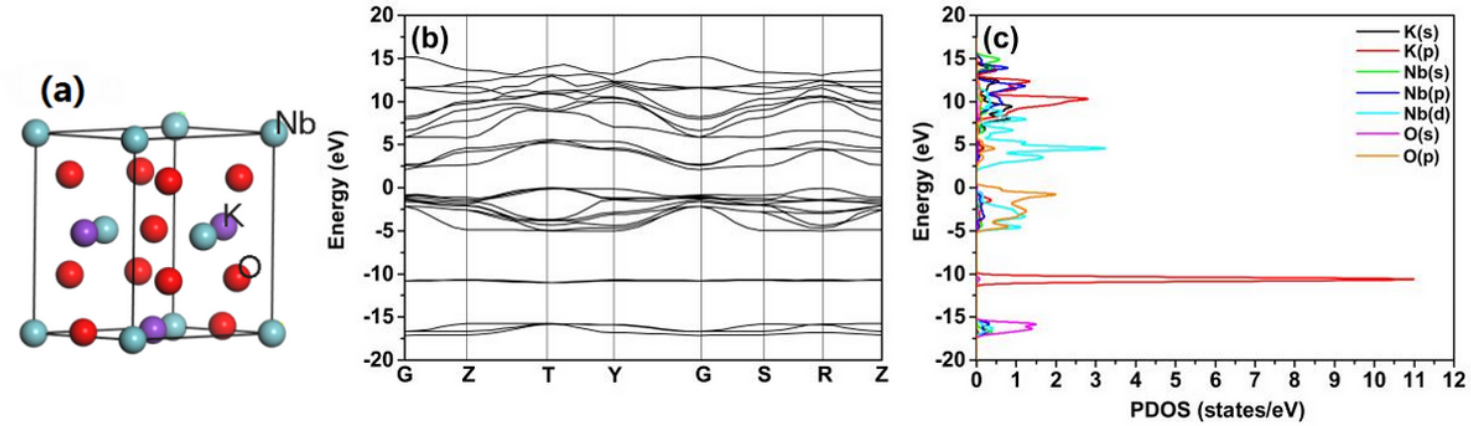

Figure 2

(a) The crystal structure of KNbO3 (KN); (b) the energy band structure and (c) the PDOS of KN piezoceramics

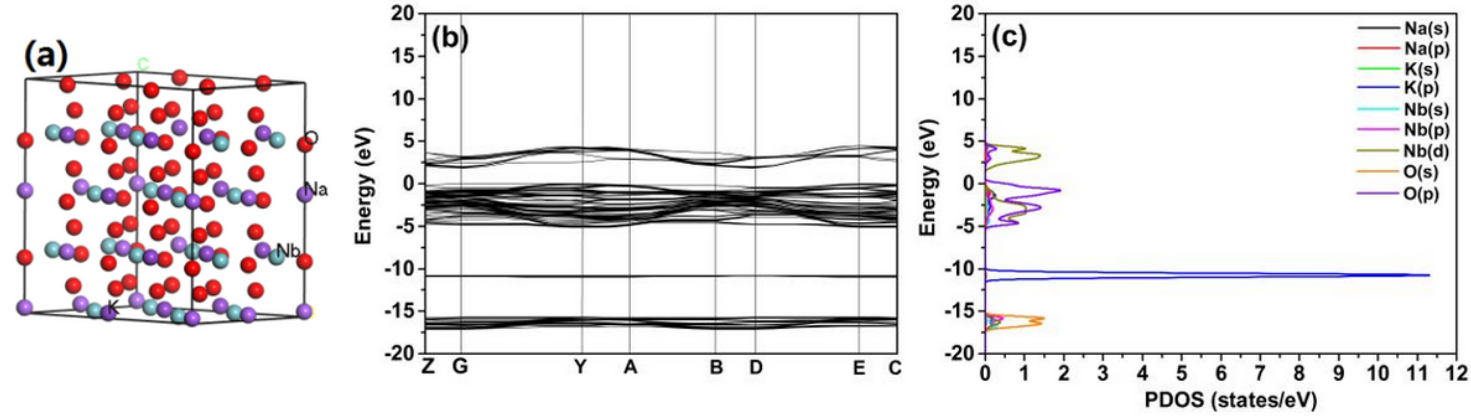

Figure 3

(a) The crystal structure of KNN; (b) the energy band structure and (c) the PDOS of KNN piezoceramics

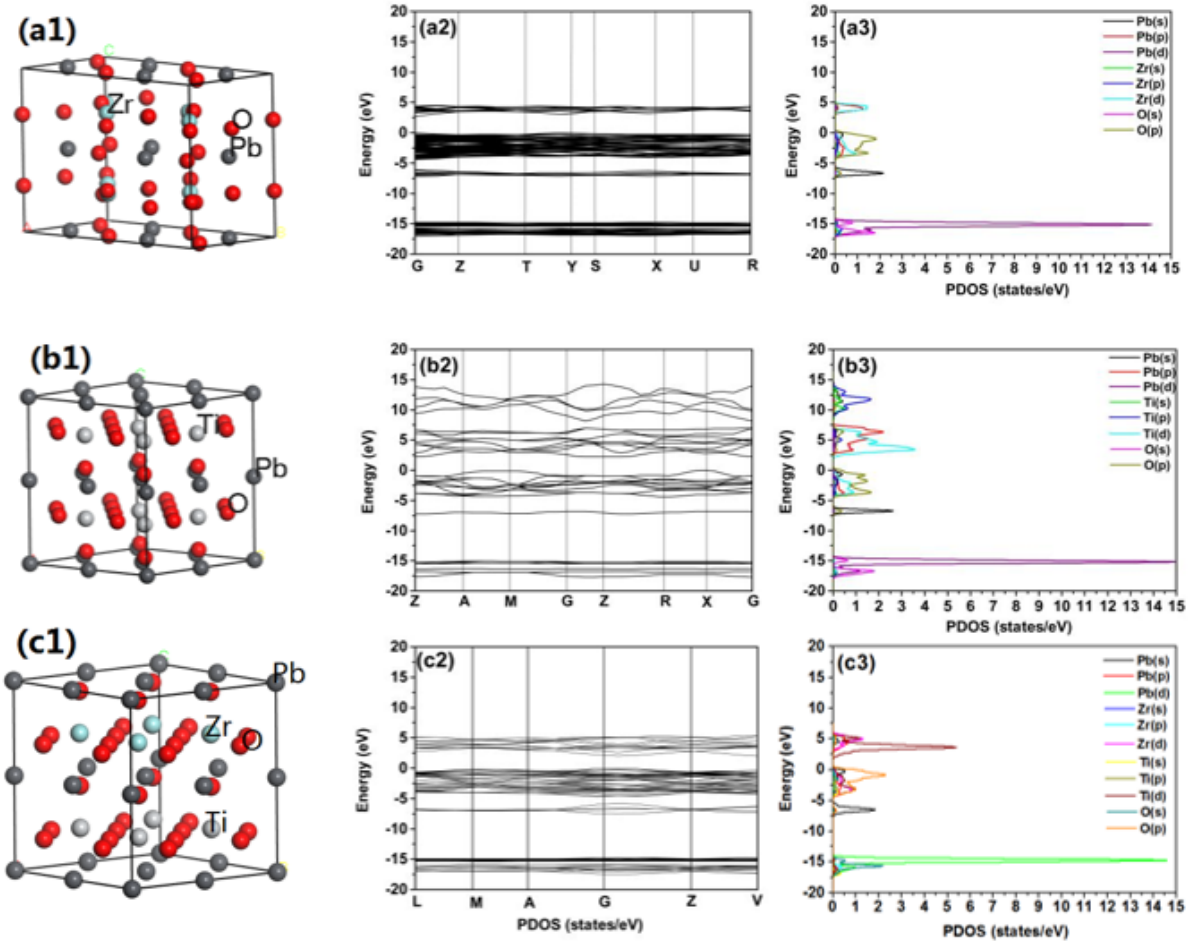

Figure 4

The crystal structure, the energy band structures and the PDOS of (a) PbZrO3 (PZ), (b) PbTiO3 (PT) and (c) PbZr0.5Ti0.5O3

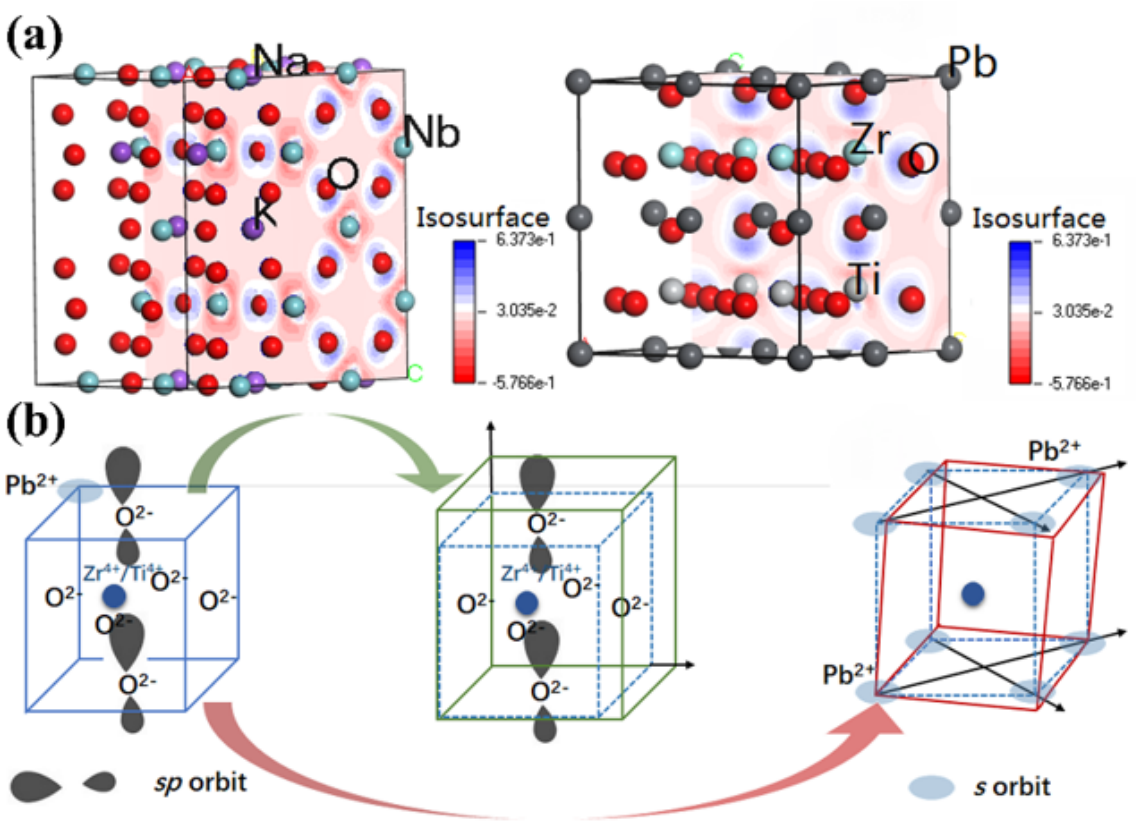

Figure 5

The electron densities of (a1) KNN and (a2) PZT; (b) the schematic of lattice deformation as well as a phase transition of PZT